Polymer Bulletin
https://doi.org/10.1007/s00289-024-05187-z

ORIGINAL PAPER

Loofah and poly(3-hydroxybutyrate-co-3-hydroxyvalerate) (PHBV) nano-fiber-reinforced chitosan hydrogel composite scaffolds with elderberry (*Sambucus nigra*) and hawthorn (*Crataegus oxyacantha*) extracts as additives for osteochondral tissue engineering applications

Gizem Baysan[1] · Pinar Akokay Yilmaz[2] · Aylin Ziylan Albayrak[1,3] · Hasan Havitcioglu[1,4]

Received: 11 September 2023 / Revised: 1 February 2024 / Accepted: 2 February 2024

Abstract

In recent years, people have had more expectations from the developed technology in medicine, especially in the field of orthopedics and traumatology. Tissue engineers are interested in techniques that benefit from patients' cells and biomaterials, instead of prostheses and implants. On the other hand, researchers have begun to use various medicinal plants for regeneration and anti-cancer studies. In the present study, we aimed to produce cartilage and bone inductive scaffolds for osteochondral tissue engineering applications with the addition of hawthorn or elderberry extracts. Firstly, wet electro-spun poly (3-hydroxybutyric acid-co-3-hydroxyvaleric acid) fibers were integrated with a loofah mat. Then, they were impregnated into chitosan solution with/without hawthorn or elderberry extract. Composite hydrogel scaffolds were obtained by cross-linking with 0.3% (*w*/*v*) genipin. Fabricated scaffolds had more than 90% porosity and showed swelling capacity in the range of 1500–2200%. Based on the in vitro biocompatibility analyses using mesenchymal stem cells (MSCs), all the fabricated scaffolds were found to be biocompatible by WST-1, ALP activity, and GAG content analysis. Also, histological/immunohistochemical analyses showed that hawthorn and elderberry extract addition increased MSCs proliferation and collagen type I and II positivity. Consequently, all the scaffolds showed promising features for osteochondral tissue engineering applications.

Extended author information available on the last page of the article

Published online: 05 March 2024

Graphical abstract

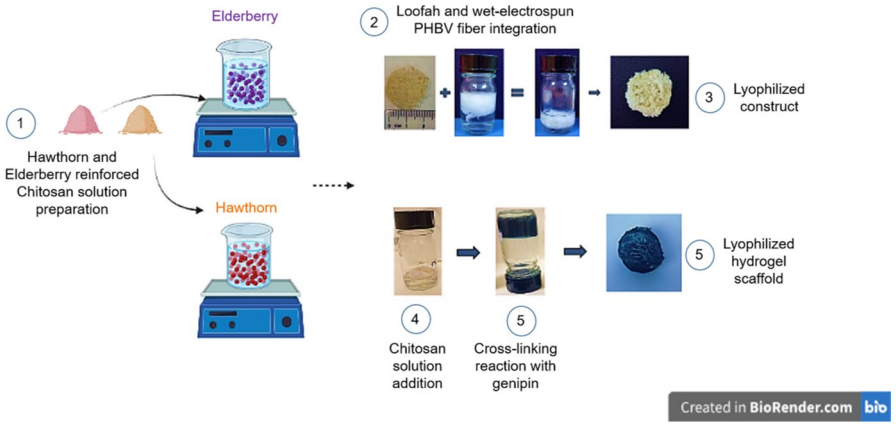

Keywords Elderberry · Hawthorn · *Luffa cylindrica* · PHBV · Hydrogel scaffold · Mesenchymal stem cells

Introduction

Ayurveda, Unani, Siddha and many other folk practices used plants widely in the treatment of various diseases. For many years, medicinal and aromatic plants have been preferred in the pharmaceutical, cosmetic, flavor, and perfumery industries. Considering all the progress in synthetic drug research, plants are still accepted as the major sources of pharmaceutical technologies [1].

Tissue engineering is a multidisciplinary field that can fulfill the functions of partially or fully damaged tissues, and aim to remodel them. Its components are composed of scaffolds produced using biomaterials, cells, biosignal molecules, and growth factors [2, 3]. In the present study, we aimed to develop a novel composite hydrogel scaffold to improve osteochondral regeneration. Osteochondral tissue defects affect both the articular cartilage and the subchondral bone tissue beneath it. These defects are generally associated with the joint' mechanical stability; also, they occur after traumatic injuries or osteochondritis dissecans [4]. In recent years, there have been many treatment methods applied such as grafting, mosaicplasty, and cell therapy. Since the articular cartilage is an avascular tissue and regenerative potential is weak, scientists continue to develop new techniques [5]. In the present study, for the first time, we aimed to use hawthorn and elderberry plant extracts in osteochondral tissue engineering applications as a scaffold ingredient due to their healing potential.

Hawthorn *(Crataegus oxyacantha)* is a member of the Rosaceae family which has been used for both medicinal purposes and nutrition. It was used effectively in Chinese medicine for many years to treat digestion, inflammation,

sugar-cholesterol level regulation, cardiovascular problems, hypertension, and kidney stones [6]. Especially, the fruits of Crataegus species are considered to be a rich source of antioxidants (isoquercetin, quercetin, etc.) with their high phenolic contents. In addition to these properties, it contains high levels of elements (Ca, K, Mg, Na and P) [7, 8].

Elderberry (*Sambucus nigra L.*) is a member of the Adoxaceae family. It was used in balancing blood pressure, reducing oxidative stress, increasing the activity of antioxidant enzymes in blood plasma including glutathione (GSH), reducing uric acid levels, hypertension, obesity, and cardiovascular diseases. Last but not least, it exhibits antiviral and antibacterial activity to support the treatment of flu and colds [9]. Elderberry is a very favorable plant in terms of both antioxidant activity (quercetin, kaempferol, isorhamnetin, etc.) and vitamins (vitamins A, B, and C). Also, it contains K, Ca, Fe, Mg, P, Na, Zn, Cu, Mn, Se, Cr, Ni, and Cd elements [10].

Luffa Cylindrica is a biodegradable, natural, and renewable plant species which is also known as loofah [11]. It has a hydrophilic fibrous structure. It is one of the medicinal plants with anticancer, antioxidant, and anti-inflammatory properties [12]. In our previous study, loofah-reinforced and wet-electrospun poly(3-hydroxybutyrate-co-3-hydroxyvalerate) (PHBV) nano-fiber-incorporated chitosan hydrogel composite scaffolds cross-linked with genipin were produced for meniscus tissue regeneration. Based on the in vitro analyses, it was found that micro- and nano-fibers promoted cell attachment and proliferation. In addition, mesenchymal stem cells (MSCs)-seeded scaffolds resulted in higher collagen type I and II immunopositivity [13]. Herein, we preferred to use this composite hydrogel scaffold design in order to investigate the effects of hawthorn and elderberry extract addition in osteochondral tissue engineering applications.

Stem cells are the cells with unlimited proliferation capacity, self-renewal ability, and differentiation potential. MSCs are multipotent stromal cells that can be isolated from most tissues (bone marrow, adipose tissue, periosteum, dental pulp, umbilical cord, synovia, etc.) and can be differentiated into various cell types such as osteocytes, chondrocytes, adipocytes, and tenocytes under suitable conditions. They are preferable alternatives for cell-based therapies due to their self-renewal potential and ability to differentiate into different cell types without tumorigenic potential [14, 15]. In this study, in vitro biocompatibility analyses were performed using MSCs to determine the differentiation potential of the produced scaffolds with/without plant extracts. Firstly, the composite hydrogel scaffolds were characterized by scanning electron microscopy (SEM) and attenuated total reflectance-Fourier transform infrared spectroscopy (ATR-FTIR) for the morphological and chemical characterizations, respectively. The swelling ratios and mechanical properties were determined by swelling and compression tests, respectively. Furthermore, cytotoxicity and cell proliferation analyses of the scaffolds were performed using WST-1 as well as ALP activity and glycosaminoglycan (GAG) contents of the scaffolds were determined for in vitro biocompatibility analyses. Histological stainings were used to observe the cells on the cross sections of the scaffolds with the Hematoxylin–Eosin (H&E), Masson Trichrome, Alcian Blue and Alizarin Red S stains. Immunohistochemical analyses were also performed to determine collagen type I and II depositions.

Materials and methods

Materials

In the study, PHBV (PHV content 3 wt%, Mn = 80 kDa) was supplied from Helian Polymers, the Netherlands. Benzyltriethylammonium chloride (BTEAC) (14,655–2), chloroform (24,216), chitosan (deacetylation degree, ≥ 75%, high molecular weight), and phosphate-buffered saline (PBS) were obtained from Sigma-Aldrich, USA. The crosslinking agent, genipin, was purchased from Wako Chemical, USA. Sodium hydroxide (NaOH) was obtained from Merck, Germany. The natural loofah plant was supplied from the Turkish Republic of Northern Cyprus region. Hawthorn extract powder (100 g; 100% natural, SYXLFDC Store) and elderberry extract powder (100 g; 100% natural, NatureHerb Store) were purchased from China. Human Mesenchymal Stem Cells (MSCs) were obtained for our previous study who underwent hip prosthesis surgery with a written consent [13]. Mesenchymal Stem Cell Growth Medium (MSCM; ScienceCell) was used in stem cell culture. StemPro Osteogenesis Differentiation Kit (Gibco, A10072-01), StemPro Chondrogenesis Differentiation Kit (Gibco, A10071-01), StemPro Adipogenesis Differentiation Kit (Gibco, A10070-01), CD 73 (APC), CD 90 (FITC), and CD 45 (PE/Cy5.5 rabbit IgG1) antibodies (Abcam) were used for mesenchymal stem cell characterizations. For cell culture, fetal bovine serum (FBS) (Cegrogen Biotech, Nordost, Germany), Trypsin–EDTA and L-glutamine (Sigma-Aldrich), penicillin–streptomycin (Invitrogen) were used as the growth supplements. Cell proliferation and viability analysis were conducted by Ready-to-use Cell Proliferation Colorimetric Reagent, WST-1 (Biovision, USA) colorimetrically. Also, glycosaminoglycan (GAG) content was measured by Blyscan, Biocolor, B1000. Finally, alkaline phosphatase activity (ALP) was measured by a colorimetric ELISA kit (FUJIFILM Wako Shibayagi Corporation, 633-51021).

Fabrication of LCPG, LCPG-H and LCPG-E scaffolds

Genipin cross-linked PHBV nano-fiber and loofah-reinforced chitosan hydrogel scaffolds (LCPG) were produced as a control group. Moreover, hawthorn or elderberry extract integrated scaffolds were produced and named as LCPG-H and LCPG-E, respectively. These scaffolds were aimed to be investigated for osteochondral tissue engineering applications.

Loofah preparation

The chemical composition of loofah (sp. *Luffa Cylindrica*) is mostly composed of holocellulose, α-cellulose, and hemicellulose and lignin [16]. Lignin is the most abundant aromatic substance in many plants. It is a polymer that is linked through C–C and C–O–C bonds to the phenylpropanoid units. Several bacteria species such as *Pseudomonas* and *Streptomyces* exhibit a broad metabolic versatility to these aromatic

substrates [17]. To eliminate the negative aspects of lignin, we treated the dried loofah with 2% NaOH for 90 min and washed with distilled water till a neutral pH was reached. Loofah was cut (30 mm diameter) and dried in a vacuum oven at 60 °C for 24 h [13]. NaOH cleans lignin and wax from the fiber surfaces and improves the mechanical properties of the loofah-reinforced composites by promoting interfacial bonding [18].

Wet electrospinning of PHBV

Before wet electrospinning of PHBV, 3% (*w*/*v*) PHBV solution was mixed with 0.2% (*w*/*v*) BTEAC and dissolved in chloroform for 2 h at 50 °C. It was stirred at RT overnight. Wet electrospun PHBV nano-fibers were collected every 15 min in a coagulation bath (9:1 v/v ethanol-distilled water) from a 10 cm working distance, a flow rate of 2.0 ml/h, and a 20 kV voltage. The wet electrospun fibers were washed with distilled water to remove ethanol [13, 19].

Chitosan solution with/without plant extract

In order to prepare 1% (*w*/*v*) chitosan solution, a high molecular weight chitosan powder was dissolved in 0.2 M acetic acid at 50 °C for 3 h which was followed by an overnight stirring at RT. The plant extract containing chitosan solutions was produced with the optimum concentration of 0.05 mg/ml hawthorn or elderberry powder, which was determined from our previous study [20]. The mixture was stirred till to get a homogeneous solution.

Obtaining LCPG, LCPG-H, and LCPG-E hydrogel scaffolds

First, the loofah mat was immersed in suspended PHBV nano-fibers. The wet electrospun PHBV nano-fibers surrounded the loofah mat and they were left overnight to integrate. Then, it was lyophilized under 0.1 bar pressure at − 25 °C for 48 h. This construct was soaked in chitosan solution to get LCPG. Furthermore, to fabricate LCPG-H and LCPH-E scaffolds, the construct was immersed in either hawthorn or elderberry-added chitosan solutions. They were lyophilized at − 60 °C for 48 h. Next, a washing step with a graded ethanol series was performed to get rid of residual acetic acid, and the construct was lyophilized. Finally, they were cross-linked using 0.3% (*w*/*v*) genipin solution for 48 h at 37 °C. The cross-linker concentration was chosen based on the results of our previous article, especially the mechanical properties [13]. The excess genipin was washed with distilled water and lyophilized again to get the final product. The loofah mat integrated hydrogel scaffolds produced had a size of 30 mm diameter and 4 mm height. However, they were cut into cylindrical samples (approximately 8 mm diameter, 4 mm height) for further analysis.

Characterization of LCPG, LCPG-H, and LCPG-E scaffolds

Scanning electron microscope (SEM) analysis

SEM (Thermo Scientific Apreo S) was used to characterize the morphological features of the LCPG, LCPG-H, and LCPG-E scaffolds. The scaffolds were sputter-coated (Leica EM ACE600) with a thin layer of Gold/Palladium to gain conductivity. The approximate pore sizes were determined with the help of the ImageJ program [21].

Attenuated total reflectance-Fourier transform infrared spectroscopy (ATR-FTIR) analysis

The chemical characterizations were performed using an ATR-FTIR (PerkinElmer Spectrum BX). Spectra were obtained in absorbance mode with a resolution of 4 cm^{-1} at 25 scans, and wavenumber ranging from 4000 to 650 cm^{-1}.

Swelling ratio analysis

The swelling ratio analysis was carried out in a PBS solution prepared by dissolving a tablet in 200 ml of distilled water and homogeneously mixing it. First, each group was studied in triplicates, and the scaffolds' dry weight was noted as w_0. The scaffolds were kept in PBS for 48 h at 37 °C. Their wet weights (w_s) at 1, 6, 24, and 48 h were noted after the excess liquid was removed by using a filter paper. The swelling ratio was calculated by using the formula below [22]:

$$\text{Swelling ratio}(\%) = \frac{\left(w_s - w_0\right)}{w_0} \times 100 \tag{1}$$

Mechanical analysis

The mechanical analyses of LCPG, LCPG-H, and LCPG-E scaffolds were performed by using a compression test in triplicates. The compressive load was applied with an electromechanical actuator (Shimadzu, 5 kN AG–X; Kyoto, Japan) with an axial load of 5 kN. The analysis was done by using a 10-mm-diameter indenter with a flat tip, at a constant strain rate of 2 mm/min up to 80% compression [23]. The force (N) and elongation (mm) values were taken from TRAPEZIUM X software. The stress (MPa)-strain (a.u.) values were processed by using the GraphPad Prism program, and the elastic modulus of the scaffolds was calculated.

In vitro biocompatibility analysis

In vitro biocompatibility analysis was performed by using passage three human bone marrow-derived mesenchymal stem cells that we produced with a primer culture from our previous study [13]. Briefly, bone marrow aspirate was taken from a hip

prosthesis surgery and MSCs were isolated by using a density gradient method with the help of Ficoll Paque solution. Flow cytometry characterizations were performed in order to prove the isolated cells were MSCs. In the present study, we investigated once more the differentiation capacities of the cells into three lineages. Cell proliferation and attachment analysis were performed after these characterizations.

Differentiation capacity of MSCs

Differentiation capacity was examined by using the 3rd passage MSCs which were seeded into 6 well-plates with a cell number of 1×10^4. Chondrogenic, osteogenic and adipogenic differentiation was studied in duplicates.

When cells became half confluent for osteogenic differentiation, they were cultured with Stempro Osteogenesis Differentiation Kit for 21 days. Then, they were fixed using a 4% formalin solution and stained with Alizarin red to histologically observe mineralization spots.

When cells became half confluent for adipogenic differentiation, they were cultured with Stempro Adipogenesis Differentiation Kit for 28 days. Then, they were fixed by using a 4% formalin solution and stained with Oil Red O to observe oil droplets histologically.

When cells became half confluent for chondrogenic differentiation, they were cultured with Stempro Chondrogenesis Differentiation Kit for 21 days. Then, they were fixed by using a 4% formalin solution and stained with Alcian blue to observe glycosaminoglycans.

In vitro biocompatibility analysis by indirect extraction method

Produced LCPG, LCPG-H, and LCPG-E scaffolds were sterilized by using ethylene oxide. They were incubated in a culture medium for 72 h at 37 °C. Trypsinized cells were seeded into 96 well plates with 1×10^3 cells/well concentration and became half confluent on 24 h. The cells were treated with the sample extracts and analyzed in triplicates at 24, 48 and 72 h. WST-1 proliferation analysis was performed according to the manufacturer's instructions to determine the viability of cells. The reaction was read colorimetrically at 450 nm absorbance by a multi-plate reader (Synergy HTX, Biotek), and the data were plotted with the help of the GraphPad Prisma program.

Cell seeding of MSCs on the hydrogel scaffolds

LCPG, LCPG-H, and LCPG-E scaffolds were cut into cylindrical samples (approximately 8 mm diameter, 4 mm height) and sterilized using ethylene oxide. MSCs were trypsinized and then counted by using a hemocytometer with trypan blue dye to determine cell viability [24]. MSCs were applied dropwise to the scaffolds at a concentration of 2×10^6 cells/ml to allow homogeneous distribution and waited an hour to attach. Then, the mesenchymal stem cell culture media was added to each well which was prepared with the addition of supplements present in the kit. They

were incubated for 28 days at 37 °C in a 5% CO_2 and 95% humidity atmosphere. Meanwhile, the medium was changed three times a week [25].

Proliferation analysis

WST-1 colorimetric ELISA test was used to determine the proliferation of MSCs on LCPG, LCPG-H, and LCPG-E scaffolds. This assay was performed on days 1, 3, 7, 14, 21, and 28 according to the manufacturer's instructions [26]. The absorbance values were taken at 450 nm wavelength with a micro-plate reader (Synergy HTX, Biotek), and the data were plotted by using the GraphPad Prisma program.

Cell attachment studies

Cell attachment of the scaffolds on days 7 and 28 was observed by using SEM after fixing with 4% formalin solution for 30 min [27]. Then, scaffolds were washed with PBS and dehydrated by a graded ethanol series (for 5 min each in 25, 50, 75, and 95% ETOH and three times 100% ETOH) [28]. The dried samples were coated by using a sputter-coater (Leica EM ACE600) and a thin layer of gold/palladium layer was coated on the scaffolds. The morphology of MSCs attached to the scaffolds was observed by Thermo Scientific Apreo S.

Determination of GAG content and ALP activity

On incubation days 7, 14, 21 and 28, the amount of GAG content [29] and ALP activity [30], which was produced due to the chondro- and osteo-inductive capacity of MSCs on the scaffolds, were measured colorimetrically with the help of ELISA kits. The analyses were performed according to the kit protocol. The color change was analyzed by a micro-plate reader with the absorbance mode at 656 nm and 405 nm wavelength for GAG and ALP, respectively.

Histological and immunohistochemical analysis

Histological and immunohistochemical analyses were performed to observe the inner structure and cellular distribution in the LCPG, LCPG-H, and LCPG-E scaffolds on day 28 of incubation. Samples were fixed with 10% formalin solution and washed under tap water overnight. Then, they were dehydrated by a graded ethanol series (for 20 min each in 70, 80, and 96%) and kept in four different acetone series for another 20 min. They were finally kept in xylene for 30 min twice and embedded in paraffin blocks. 5 µ thickness sections were cut by a microtome (RM 2255, Leica). Hematoxylin & Eosin (H&E) for general morphology, Masson trichrome (MT) for collagen deposits, Alcian blue (AB) for glycosaminoglycan structures and Alizarin Red S for mineralization were performed to evaluate histologically. Moreover, type I and type II collagen antibodies were used to determine collagen production of the scaffolds to evaluate bone and cartilage formation, respectively. The sections were examined by using a light microscope (Olympus BX-51 Tokyo, Japan), and the images were taken with a

high-resolution camera (Olympus DP-71, Japan). 5 sites for each sample were observed, and sections were excluded with obvious artifacts because of the inconvenient staining. A computerized video camera-based image analysis (UTHSC Image software) method was used for examining the cross-sectional images.

Statistical analysis

The results were statistically analyzed as mean ± standard error of at least three replicates. The statistical analysis was performed by using a two-way analysis of variance (ANOVA) test. For multiple comparisons, post hoc Tukey's test was used. The statistically significant value was considered as $p \leq 0.05$.

Results and discussion

Fabrication of LCPG, LCPG-H and LCPG-E scaffolds

A novel genipin cross-linked PHBV nano-fiber and loofah-reinforced chitosan hydrogel scaffolds with/without hawthorn and elderberry extract were fabricated, and the fabrication process is shown in Fig. 1. At first, the loofah mats (30 mm in diameter) were washed and dried (Fig. 1a). Meanwhile, PHBV nano-fibers were produced by using the wet electrospinning method (Fig. 1b). The loofah mat was successfully surrounded by PHBV nano-fibers (Fig. 1c) and lyophilized (Fig. 1d). The obtained constructs were soaked in chitosan, chitosan/hawthorn and chitosan/elderberry solutions (Fig. 1e), lyophilized, and then cross-linked by using 0.3% (*w*/*v*) genipin solution for 48 h to get LCPG, LCPG-H, and LCPG-E composite hydrogels, respectively (Fig. 1f). The excess genipin was washed away, and a final lyophilization step was performed to get the composite hydrogel scaffolds (Fig. 1g–i).

Chitosan was preferred as the hydrogel matrix due to its structural similarity with the glycosaminoglycan and hyaluronic acid found in articular cartilage. It is a promising polymer for cartilage and osteochondral regeneration with its biocompatible, biodegradable, and antibacterial features [31]. On the other hand, as the nanofibrous structure, PHBV was used as it has good spinnability under wet-electrospinning conditions as well as it is biocompatible and biodegradable [34]. In our previous studies, wet electrospun PHBV nanofibers were used together with the macro-fibrous loofah mat in the design of scaffolds for both meniscus and osteochondral tissue regeneration [13, 32]. These fibrous structures not only reinforced the hydrogels but also, they became favorable sites for cell attachment. Moreover, it is stated in the literature that in damaged cartilage, antioxidants may help reduce the high level of reactive oxygen species (ROS) produced by the chondrocytes to maintain cartilage homeostasis [33]. Thus, using antioxidant-rich hawthorn and elderberry extracts as scaffold additives is a promising approach to enhance osteochondral healing.

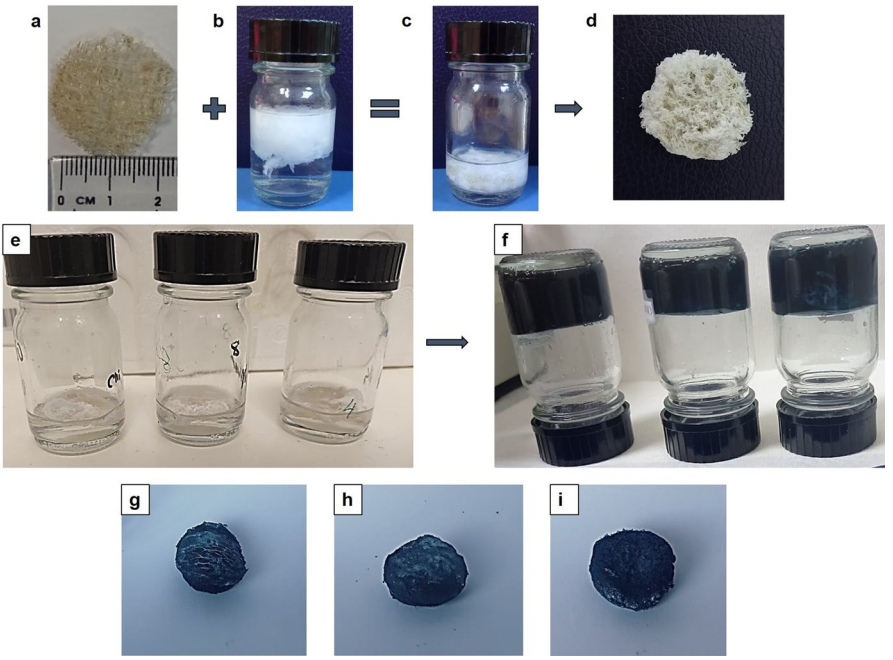

Fig. 1 Fabrication of the composite hydrogel scaffolds. **a** Washed and dried loofah mat, **b** wet electrospun PHBV nano-fibers, **c** the loofah mat immersed in suspended PHBV nano-fibers, **d** PHBV nano-fiber integrated loofah mat after lyophilization. **e** From left to right, Loofah/PHBV construct soaked in chitosan, chitosan/hawthorn, and chitosan/elderberry solutions. **f** From left to right, LCPG, LCPG-H, and LCPG-E composite hydrogels after genipin cross-linking reaction. **g** LCPG, **h** LCPG-H, and **i** LCPG-E scaffolds at the end of the final lyophilization step

Characterization of LCPG, LCPG-H, and LCPG-E scaffolds

Scanning electron microscope (SEM) analysis

Scaffold porosity plays an important role in the regulation of cellular growth and viability. The cell response changes depending on the intercellular communication. The high porosity rate and interconnected open porous structure of the scaffolds enable homogeneous nutrient and gas diffusion in the inner structure. In addition, pore size and morphology vary with the polymer type, fabrication method, and cross-linker ratio. Although the minimum porosity required for cell adhesion and proliferation in a scaffold is stated as 50%, it is known that the ideal ratio is at least 90%. In osteochondral tissue engineering, the ideal pore size of scaffolds should be in the range of 50–350 µm for chondrogenesis [34, 35]. When the results are considered, LCPG, LCPG-H, and LCPG-E scaffolds had open porosity and the percent porosity was more than 90% for each. Mean pore sizes were calculated from ten different regions with the ImageJ program and the average pore sizes for LCPG, LCPG-H, and LCPG-E scaffolds were 114.25 ± 13.85,

125.38 ± 12.10, and 167.93 ± 18.62 µm, respectively. Also, as shown in Fig. 2, the loofah mat and PHBV nano-fibers were well integrated into the structure. With all this information, it can be stated that the morphology of all the scaffolds was convenient for osteochondral tissue engineering applications.

Attenuated total reflectance-Fourier transform infrared spectroscopy (ATR-FTIR) analysis

LCPG, LCPG-H, and LCPG-E scaffolds' chemical structures were analyzed by using ATR-FTIR (Fig. 3a and b). Characteristic peaks of chitosan polymer in the scaffolds were at ~ 3299–3281 cm^{-1} (O–H and N–H stretching bands), ~ 2883 cm^{-1} (C–H stretching band), ~ 1645 cm^{-1} (C=O stretching band of the amide group), ~ 1558 cm^{-1} (N–H bending band of the amine group), ~ 1066 cm^{-1} (C–O stretching band), and ~ 1028 cm^{-1} (C–O–C stretching band). After the NaOH treatment of loofah, the characteristic peaks can be observed at ~ 3335 cm^{-1} (O–H stretching band), ~ 2921 cm^{-1} (C–H stretching band), ~ 1421 cm^{-1} (CH_2 bending band of cellulose), and ~ 1153 cm^{-1} (C–O–C asymmetric bridge of cellulose stretching band), while the peaks of hemicellulose (~ 1735 cm^{-1}, C=O stretching band) and lignin (~ 1470 cm^{-1}) were disappeared as expected. The characteristic peaks of PHBV fibers were at ~ 2930 cm^{-1} (C–H stretching vibration band), 1722 cm^{-1} (C=O stretching band), ~ 1455 and 1380 cm^{-1} (C–H bending bands), and ~ 1280 and 1055 cm^{-1} (C–O stretching bands). Genipin characteristic peaks were indicated as ~ 1680 cm^{-1} (ester group, C=O stretching band), ~ 1620 cm^{-1} (C=C stretching band), ~ 080 cm^{-1} (C–O stretching band) [13]. As a result of the FTIR analysis performed on the LCPG scaffold, the related absorbance bands of the components in the scaffold were seen at ~ 3262, 2921, 1722, 1634, 1545, 1378, 1309, 1151, 1058, and 1034 cm^{-1}. Finally, due to the cross-linking reaction between genipin and chitosan, the C=O band which is at ~ 1645 cm^{-1} was observed to be shifted to ~ 1634 cm^{-1}

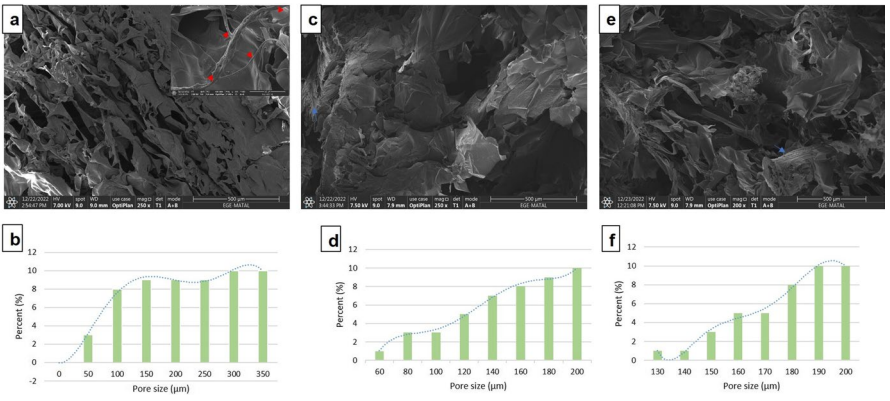

Fig. 2 Cross-sectional images of **a** LCPG, **c** LCPG-H, and **e** LCPG-E scaffolds with 500 × magnification. Histograms of the pore size distribution for **b** LCPG, **d** LCPG-H, and **f** LCPG-E scaffolds. Red arrows show PHBV nano-fibers and blue arrows the loofah fibers (color figure online)

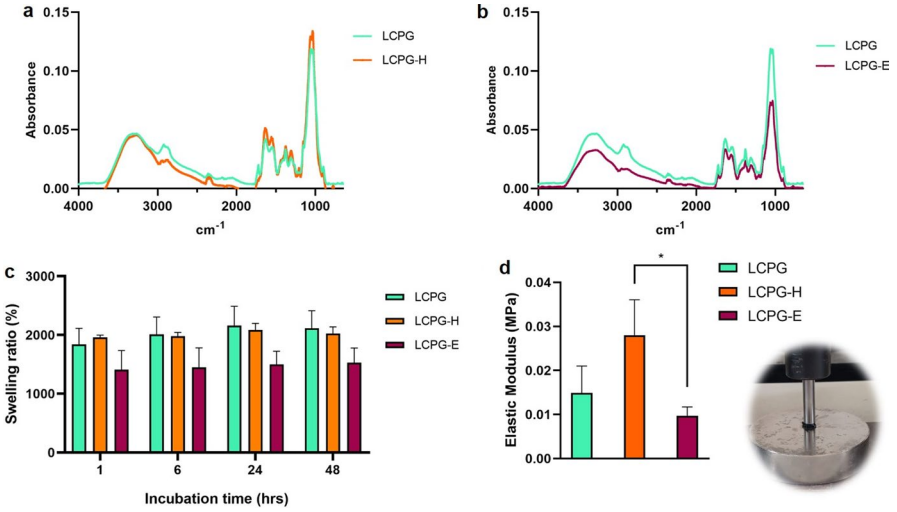

Fig. 3 **a** FTIR spectrum of LCPG and LCPG-H scaffold. **b** FTIR spectrum of LCPG and LCPG-E scaffold. **c** Swelling ratio analysis of LCPG, LCPG-H and LCPG-E scaffolds. **d** Mechanical compression test results of LCPG, LCPG-H and LCPG-E scaffolds (left side) and the test set-up (right side) (*$p < 0.05$)

with the formation of secondary amide band. The reaction mechanism was depicted in our previous study, in detail [13].

FTIR analyses of the LCPG-H and LCPG-E scaffolds containing hawthorn and elderberry extracts are shown in Fig. 3a and b, respectively. In addition to the peaks of LCPG scaffold, the characteristic peaks of the hawthorn extract were seen at ~ 3297 cm^{-1} (intermolecular O–H hydrogen bonding), ~ 2922 cm^{-1} (C–H stretching band), and ~ 1013 cm^{-1} (C–O stretching band) [36]. Furthermore, C=C vibration bands belonging to the aromatic groups were observed at ~ 1645 and 1457 cm^{-1} [37]. The characteristic peaks of the elderberry extract were seen at ~ 3332 cm^{-1} (O–H stretching band), ~ 2929 cm^{-1} (C–H stretching band), ~ 1715 cm^{-1} (C=O stretch band), and ~ 1645 cm^{-1} (C=C aromatic group band) [38, 39]. As a result, when the FTIR spectra of the LCPG-H and LCPG-E scaffolds were compared with that of the LCPG scaffold, ~ 1645 cm^{-1} peak was found to be distinctive as an indication of plant extract addition. From the graphs, it can be concluded that hawthorn and elderberry plants were successfully added to the scaffolds, and the cross-linking reaction was completed.

Swelling ratio analysis

The water binding capacity of LCPG, LCPG-H, and LCPG-E scaffolds was determined by swelling analysis in PBS. This analysis is vital for both hydrogels and other biodegradable biomaterials. It gives clues about the scaffold's physical properties. The swelling capacity is not only important for the absorption of body fluids, but also the transfer of nutrients and metabolites. It is expected that the cells will bind to the hydrophilic scaffold surface better and migrate [40].

Considering our results, all the scaffolds had a high and rapid swelling tendency due to the interconnected porous structure of the scaffolds along with the hydrophilic nature of chitosan and loofah. The average swelling ratios at 24 h were calculated approximately as 2162%, 2083.57%, and 1498.85% for the LCPG, LCPG-H, and LCPG-E scaffolds, respectively (Fig. 3c). The obtained data were relevant to the chitosan-based scaffolds present in the literature [40]. Even though the LCPG and LCPG-H scaffolds had a similar swelling ratio, the LCPG-E scaffold showed a lower swelling trend. However, the decrease was found to be statistically insignificant.

Mechanical analysis

The compression modulus of the human cartilage is in the range of 240–1000 kPa [41]. Moreover, bone tissue consists of organic and inorganic components in an anisotropic structure. Its mechanical properties vary, for example, the transverse elastic modulus and the longitudinal modulus of cortical bone are 10.1 ± 2.4 GPa and 17.9 ± 3.9 GPa, respectively. Trabecular bone tissue, on the other hand, performs better strength to compression loading than tensile loading. The compressive modulus is in the range of 1–900 MPa [42]. The average compressive moduli of the LCPG, LCPG-H, and LCPG-E scaffolds were around 0.015, 0.028, and 0.01 MPa, respectively (Fig. 3d). The statistical analysis showed no significant difference among LCPG/LCPG-H and LCPG/LCPG-E scaffolds. However, there is a statistically significant difference between LCPG-H and LCPG-E scaffolds ($p = 0.0218$). LCPG-H scaffold was more brittle than the others due to its higher compression modulus. The compression analysis result of the LCPG-E scaffold was correlated well with its higher pore size distribution resulting in its lower mechanical properties. However, the heterogeneous distribution of the micro-fibers within the natural loofah mats should also be considered as it increased the standard deviation of the samples. Even though the compression moduli of the scaffolds seemed to be lower for the osteochondral tissue engineering, considering the range of moduli of elasticity for soft tissues, which ranged from several kPa to MPa [43], our fabricated scaffolds' moduli were closer to that of cartilage and trabecular bone tissue. By considering the structure and mechanical properties of osteochondral tissue which vary from the cartilage surface to the subchondral bone tissue, composite materials with a fibrous architecture seem to be a better option as scaffolding materials for osteochondral tissue engineering applications. The fabricated scaffolds' mechanical properties may be improved by additional fiber reinforcement.

In vitro biocompatibility analyses

This study used a P3 human mesenchymal stem cell line that was previously isolated from bone marrow aspirate with the approval of a local ethics committee of Dokuz Eylul University, Noninvasive Medical Researches (protocol number: 3322-GOA). In vitro biocompatibility analyses were performed in two steps. Firstly, a basic cytotoxicity test which is called the "indirect extraction method" was applied. Then, in vitro biocompatibility analyses were performed by seeding MSCs on the LCPG, LCPG-H, and LCPG-E hydrogel scaffolds.

Differentiation capacity of MSCs

As aforementioned, MSCs were incubated and observed with an inverted microscope for 21 and 28 days. At the end of this culture period, they were stained by using Alcian Blue, Alizarin Red S, and Oil Red O dyes to confirm that they were differentiated into chondrogenic, osteogenic, and adipogenic lineages, respectively. Chondrogenic cells were stained intensely blue (Fig. 4a), while other sites were lightly stained. Besides, osteogenic cells were stained in bright orange color which indicated the extracellular calcium deposits (Fig. 4b). Finally, adipogenic cells were stained in bright red color which also showed lipid morphology (Fig. 4c).

In vitro biocompatibility analysis by indirect extraction method

After the ethylene oxide sterilization of LCPG, LCPG-H, and LCPG-E scaffolds, they were incubated in a culture medium for 72 h at 37 °C. Sample extracts were taken and kept in 4 °C. Also, 1×10^3 cells/well were seeded into 96 well plates and waited to become half confluent. After 24 h of incubation with the MSC growth medium, cells were treated with the sample extracts. WST-1 proliferation analyses were performed at 24, 48 and 72 h colorimetrically, and the data were plotted (Fig. 4d).

All the three scaffolds showed no cytotoxic effect. LCPG-H and LCPG-E scaffolds showed slightly more proliferation ratios when compared to LCPG scaffolds,

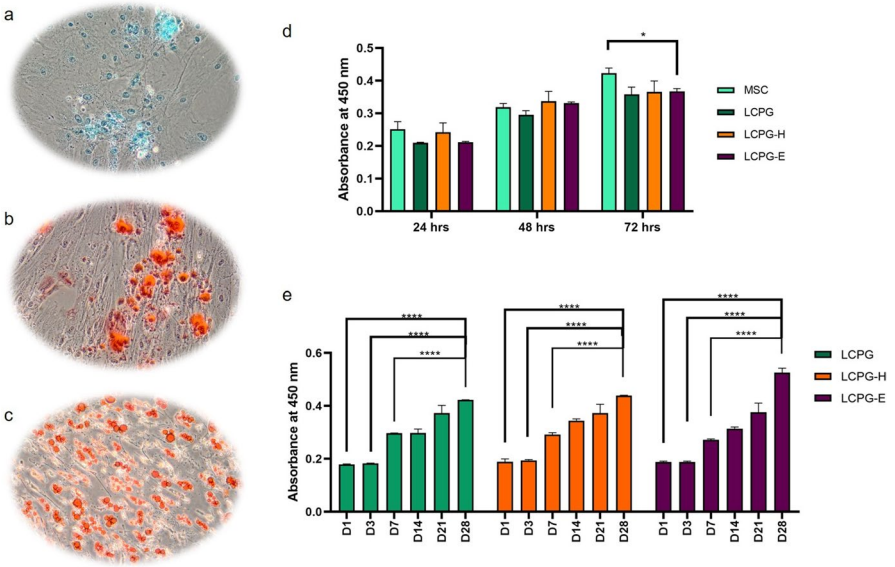

Fig. 4 Differentiation analysis of MSCs **a** Alcian Blue staining for chondrogenic. **b** Alizarin Red S staining for osteogenic, and **c** Oil Red O staining for adipogenic differentiation. **d** WST-1 proliferation analysis of LCPG, LCPG-H, and LCPG-E scaffolds by indirect extraction method. **e** WST-1 proliferation analysis for 28 days of incubation with MSCs (*$p < 0.05$ and ****$p < 0.0001$)

especially for 48 h of incubation. However, there was no statistically significant difference between the three scaffolds. Only elderberry extract added scaffold (LCPG-E) showed a significant difference ($p = 0.0337$) at 72 h of incubation when compared to the MSCs. The detailed biocompatibility analyses were performed by seeding cells with a density of 2×10^6 cells/ml on the scaffolds and incubating for 28 days.

Proliferation analysis

MSCs were cultured for 28 days, and the proliferation analyses were performed on days 1, 3, 7, 14, 21, and 28. The absorbance values were taken at 450 nm and plotted by using the graphpad program (Fig. 4e). On days 1 and 3, the proliferation values were similar for all the groups, but the absorbance values were lower than expected. This might be due to the release of genipin into the culture media. Even though genipin is considered as a low-toxic cross-linker, researchers developed an increasing interest in the use of genipin which is extracted from the gardenia fruit, as a natural cross-linker for the primary amino group containing polymers such as chitosan [44]. After the 7th day of incubation, there occurred a parabolic increase for all the groups. Also, the proliferation rates for LCPG-H and LCPG-E scaffolds were higher than LCPG. The highest metabolic activity was measured at the 450 nm absorbance value of 0.423, 0.439 and 0.526 for LCPG, LCPG-H, and LCPG-E scaffolds on the 28th day of incubation, respectively. The statistical analysis at 28th day of incubation indicated that the LCPG-E scaffold showed a significant difference between LCPG ($p < 0.0001$) and LCPG-E ($p < 0.0001$).

This sudden increase in LCPG-E scaffold might be due to the release of elderberry extract increasing the proliferation capacity. Also, there might be the differentiation of MSCs on the scaffolds and this might increase the proliferation, especially on day 28. Various stages of differentiation affect proliferation differently [45]. However, this analysis was not enough to confirm the differentiation; therefore, histological/immunohistochemical analysis was required. As a result, all three scaffolds could be accepted as non-cytotoxic, and hawthorn or elderberry extract addition to the scaffolds were considered promising in terms of cell proliferation.

Cell attachment studies

General morphology and cell attachment were observed by using SEM analysis. SEM images were taken on the 7th and 28th days of incubation for LCPG, LCPG-H, and LCPG-E scaffolds. It was observed that MSCs adhered to the surface of all the three scaffolds and distributed homogeneously [46]. It was depicted that the cells adhered especially to the micro- and nano-fiber surfaces, formed clusters, and extended into the pores. Most of the cells on the surfaces were round-shaped. On day 28, it is seen that the cells proliferated and spread over the surface more than on day 7 (Fig. 5). The attached cells were rounder, especially in the LCPG-E scaffolds. We believe that extract addition triggered the chondrogenic differentiation of MSCs [47]. Meanwhile, the control group (LCPG) showed cellular extensions more like fibroblastic cells. Moreover, bridge-like structures that appeared in the images are

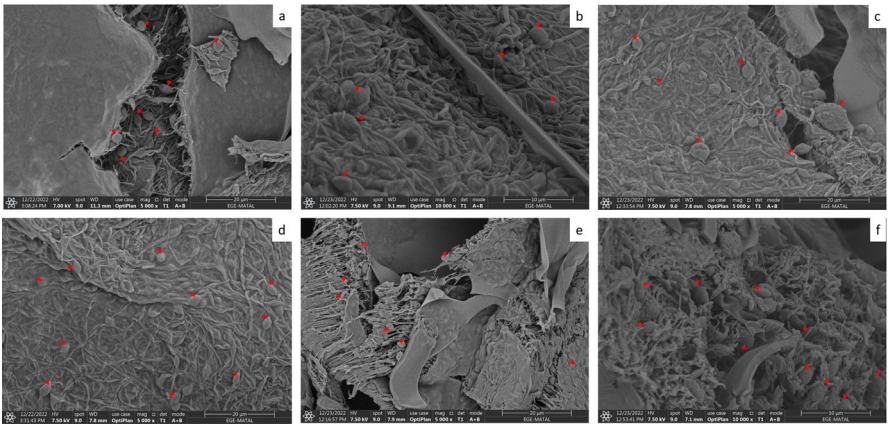

Fig. 5 SEM images of MSCs seeded scaffolds: **a** LCPG, **b** LCPG-H, **c** LCPG-E on day 7; **d** LCPG, **e** LCPG-H, and **f** LCPG-E on day 28 with 5000 × and 10,000 × magnifications. The red arrows show cells attached to the surface (color figure online)

expected to increase cell–cell interactions, contact-based signaling, and nutrient and gas exchange.

Determination of GAG content and ALP activity

ALP activity analysis was performed to determine the osteogenic differentiation of MSCs seeded in LCPG, LCPG-H, and LCPG-E scaffolds (Fig. 6a). ALP activity was measured using p-nitrophenyl phosphate (pNPP) as the substrate (which converts p-NPP to para-nitrophenol (p-NP) and causes the color to change to yellow). This enzyme catalyzes the hydrolysis of phosphate monoesters from many molecules at basic pH and plays an indispensable role in phosphate metabolism [48]. In the present study, the used MSCs only consist of osteoblast precursor cells and

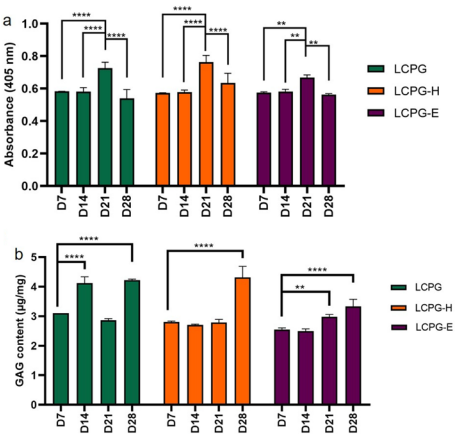

Fig. 6 On days 7, 14, 21, and 28 of incubation with mesenchymal stem cells **a** ALP activity and **b** GAG content analysis of LCPG, LCPG-H, and LCPG-E scaffolds (**$p < 0.01$ and ****$p < 0.0001$)

do not include the hematopoietic lineage-derived osteoclasts or osteoclast-like cells. The higher pH is likely related to the viability of osteoblasts with the increased ALP activity and the maturation of the MSCs [49]. It is seen that there is a statistically significant increase in the amount of ALP for all the groups until day 21. The LCPG-H scaffold had slightly higher absorbance values when compared to the others on days 21 and 28 in correlation with its higher elastic modulus. This situation is directly related to the increase in the population of osteogenic cells.

Proteoglycans form 5 to 10% of the cartilage wet weight and play a vital role in the load-bearing mechanisms of articular cartilage tissue. They are macromolecules that can attach to a protein core with hundreds of GAGs, and the most abundant form of them is chondroitin sulfate. The charged groups (sulfate and carboxyl) on GAGs are responsible for the Donnan osmotic pressure that provides the compressive stiffness of cartilage tissue. In addition, due to their hydrophilic structure, proteoglycans play an important role, by restricting the water flow, in the biphasic lubrication mechanism of cartilage. The pressurized interstitial water content of the cartilage absorbs most of the load applied to the cartilage surface at the initial loading and thus reduces the subsequent friction force. This interaction between proteoglycans, interstitial water content, and the collagen network of cartilage is crucial for the proper biomechanical function and lubrication mechanisms of articular cartilage [50]. That is why, it is quite important to measure the GAG content in cartilage scaffolds. In the present study, to determine the chondrogenic differentiation of MSCs biochemically, GAG content was analyzed with DMMB assay (Fig. 6b). All the scaffolds had the maximum GAG content on the 28th day of the incubation period (4.23, 4.31, and 3.33 µg/mg for LCPG, LCPG-H, and LCPG-E, respectively), which was statistically significant ($p < 0.0001$) when compared to day 7. When we compare the sulfated GAG amount (µg/mg) per scaffold, it is seen that scaffolds allowed new GAGs to be formed. The data are consistent with the results of chitosan-based scaffolds (approximately 10 µg/mg) [51], but insufficient for human cartilage tissue (approximately 50 µg/mg) [52]. If the culture period had extended or a dynamic culture had been performed, we could have achieved a better GAG content ratio.

Histological and immunohistochemical analysis

It is known from the literature that chitosan polymer with biomimetic features is preferred for osteochondral tissue engineering [53, 54]. When histological and immunohistochemical analyses were examined, elderberry and hawthorn extract added scaffolds supported the proliferation of cells (Fig. 7). Also, the cells mostly preferred to accumulate around the loofah fibers. In H&E staining, the general morphology was observed, and it was observed that the cells were distributed well inside the pores of the scaffolds. We performed the Alcian Blue and Alizarin Red S stainings to observe GAG structures and mineralization, respectively. All the three scaffolds were stained well which is also relevant to the biochemical results for GAG content and ALP activity analysis. The extract added groups stained slightly darker for both stainings. In Masson Trichrome staining, the amount of collagen was compared among the groups. Accordingly, a more homogeneous collagen structure was detected in the LCPG + H group.

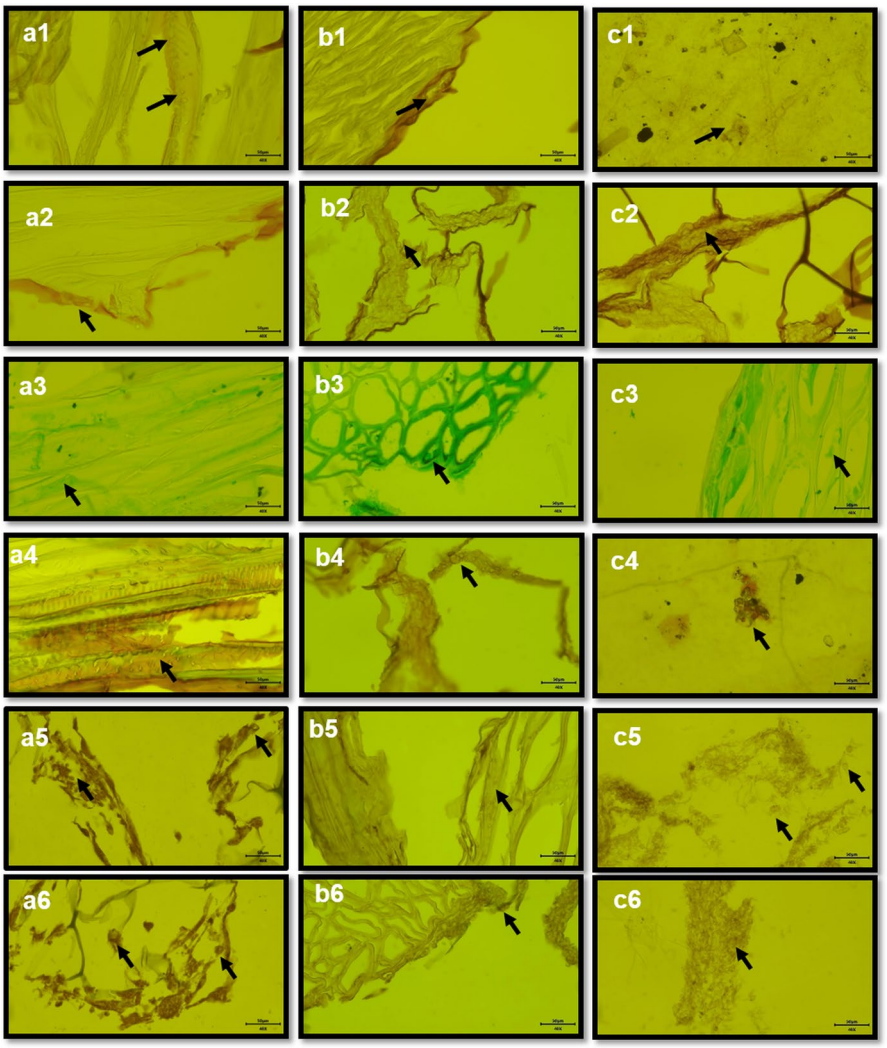

Fig. 7 Histological and immunohistochemical analysis of **a** LCPG, **b** LCPG-H, and **c** LCPG-E scaffolds. H&E staining (a1, b1, c1), Alizarin Red S staining (a2,b2, c2), Alcian Blue staining (a3, b3, c3), Masson Trichrome staining (a4, b4, c4), Type I collagen staining (a5, b5, c5), Type II collagen staining (a6, b6, c6). 40X magnification with a scale bar of 50 µm. The cells were indicated with black arrows

Besides, immunohistochemical analyses depicted that extract addition increased collagen type I and II formation. The results showed that hawthorn and elderberry extracts are promising additives to the scaffolds for osteochondral tissue engineering applications.

Conclusion

In this study, genipin cross-linked PHBV nano-fiber and loofah-reinforced chitosan hydrogel scaffolds (LCPG) were fabricated with/without the addition of hawthorn or elderberry extracts for osteochondral tissue engineering applications. Material characterizations and in vitro biocompatibility analyses with MSCs were performed on LCPG, LCPG-H, and LCPG-E scaffolds.

The fabricated scaffolds had enough porosity for chondrogenesis and showed a high swelling capacity. Based on the compression test results, the scaffolds had mechanical features with a biomimicking potential better for cartilage tissue than osteochondral tissue. The in vitro biocompatibility analysis showed that all the three scaffolds were non-cytotoxic and the scaffolds with micro- and nano-fiber surfaces were suitable for MSCs to attach and adhere. Besides, the hawthorn and elderberry extract addition to the LCPG scaffold increased cell proliferation, especially elderberry. Moreover, biochemical ALP activity and GAG content analysis showed that all the scaffolds were suitable for osteochondral tissue engineering applications. In addition, histological stainings and immunohistochemical analysis depicted that hawthorn and elderberry extract added scaffolds supported MSCs proliferation as well as collagen type I and II positivity.

As a result, all the fabricated scaffolds were found to be biocompatible. The results showed that hawthorn and elderberry extract addition with an antioxidant potential is a promising approach for osteochondral tissue engineering. Furthermore, in vivo biocompatibility and pre-clinical studies should be carried out to determine the effects of these extracts for osteochondral tissue regeneration.

Acknowledgements The author (Gizem Baysan) was a scholar in the Council of Higher Education (YOK) 100/2000 Doctoral Program in the thematic field of Biomaterials and Tissue Engineering. The authors are grateful to Ege University, Central Research Test and Analysis Laboratory Application and Research Center (Ege-MATAL) for the SEM analysis.

Funding Open access funding provided by the Scientific and Technological Research Council of Türkiye (TÜBİTAK).

Declarations

Conflict of interest The authors declare that there are no known competing financial interests or personal relationships that influence the work reported in this paper.

References

1. Swamy MK, Sinniah UR (2015) A comprehensive review on the phytochemical constituents and pharmacological activities of *Pogostemon cablin* Benth.: an aromatic medicinal plant of industrial importance. Molecules 20:8521–8547. https://doi.org/10.3390/molecules20058521
2. Chan BP, Leong KW (2008) Scaffolding in tissue engineering: general approaches and tissue-specific considerations. Eur Spine J. https://doi.org/10.1007/s00586-008-0745-3
3. Abdelaziz AG, Nageh H, Abdo SM et al (2023) A review of 3D polymeric scaffolds for bone tissue engineering: principles, fabrication techniques, immunomodulatory roles, and challenges. Bioengineering 10(2):204. https://doi.org/10.3390/bioengineering10020204
4. Martin I, Miot S, Barbero A et al (2007) Osteochondral tissue engineering. J Biomech 40:750–765. https://doi.org/10.1016/j.jbiomech.2006.03.008
5. Wei W, Dai H (2021) Articular cartilage and osteochondral tissue engineering techniques: recent advances and challenges. Bioact Mater 6:4830–4855. https://doi.org/10.1016/j.bioactmat.2021.05.011
6. Rigelsky JM, Sweet BV (2002) Hawthorn: pharmacology and therapeutic uses. Am J Heal Pharm 59:417–422. https://doi.org/10.1093/ajhp/59.5.417
7. Alirezalu A, Ahmadi N, Salehi P et al (2020) Physicochemical characterization, antioxidant activity, and phenolic compounds of hawthorn (*crataegus* spp.) fruits species for potential use in food applications. Foods 9(4):436. https://doi.org/10.3390/foods9040436
8. Özcan M, Haciseferoğullari H, Marakoğlu T, Arslan D (2005) Hawthorn (*Crataegus* spp.) fruit: some physical and chemical properties. J Food Eng 69:409–413. https://doi.org/10.1016/j.jfoodeng.2004.08.032
9. Sidor A, Gramza-Michałowska A (2015) Advanced research on the antioxidant and health benefit of elderberry (*Sambucus nigra*) in food—a review. J Funct Foods 18:941–958. https://doi.org/10.1016/j.jff.2014.07.012
10. Młynarczyk K, Walkowiak-Tomczak D, Łysiak GP (2018) Bioactive properties of *Sambucus nigra* L. As a functional ingredient for food and pharmaceutical industry. J Funct Foods 40:377–390. https://doi.org/10.1016/j.jff.2017.11.025
11. Ighalo J (2023) Comparing the effect of mercerisation, acetylation and oxidation on the tensile properties of *Luffa Cylindrica* fibers. Jordanian J Eng Chem Ind 6:21–25. https://doi.org/10.48103/jjeci642023
12. Bharathidasan P, Priya VV, Gayathri R, Kavitha S (2023) Biogenic selenium nanoparticles loaded alginate-gelatin scaffolds for potential tissue engineering applications experimental section fabrication of SeNPs Loaded AlgGel. https://doi.org/10.21522/TIJPH.2013.SE.23.01.Art010
13. Baysan G, Colpankan O, Akokay P et al (2022) International journal of biological macromolecules (PHBV) based hydrogel scaffolds for meniscus tissue engineering applications. Int J Biol Macromol 221:1171–1183. https://doi.org/10.1016/j.ijbiomac.2022.09.031
14. Ding DC, Shyu WC, Lin SZ (2011) Mesenchymal stem cells. Cell Transpl 20:5–14. https://doi.org/10.3727/096368910X
15. Bianco P (2014) Mesenchymal stem cells. Annu Rev Cell Dev Biol 30:677–704. https://doi.org/10.1146/annurev-cellbio-100913-013132
16. Tanobe VOA, Sydenstricker THD, Munaro M, Amico SC (2005) A comprehensive characterization of chemically treated Brazilian sponge-gourds (*Luffa cylindrica*). Polym Test 24:474–482. https://doi.org/10.1016/j.polymertesting.2004.12.004
17. Rafael V (1988) Bacterial degradation of lignin. Enzyme Microb Technol 10:646–655. https://doi.org/10.1016/0141-0229(88)90055-5
18. Ubi PA, Abdul S, Asipita R (2015) Effect of sodium hydroxide treatment on the mechanical properties of crushed and uncrushed *Luffa Cylindrica* fibre reinforced rLDPE composites. Int J Mater Metall Eng 9:203–208
19. Gunes OC, Albayrak AZ, Tasdemir S, Sendemir A (2020) Wet-electrospun PHBV nanofiber reinforced carboxymethyl chitosan-silk hydrogel composite scaffolds for articular cartilage repair. J Biomater Appl 35:515–531. https://doi.org/10.1177/0885328220930714
20. Baysan G, Husemoglu RB, Havıtçıoğlu H (2020) Cytotoxic effects of hawthorn and elderberry extracts on 3T3 fibroblast cell line. J Med Innov Technol 2:85–91

21. Baniasadi H, Ramazani SAA, Mashayekhan S (2015) Fabrication and characterization of conductive chitosan/gelatin-based scaffolds for nerve tissue engineering. Int J Biol Macromol 74:360–366. https://doi.org/10.1016/j.ijbiomac.2014.12.014
22. Mh Busra F, Rajab NF, Tabata Y et al (2019) Rapid treatment of full-thickness skin loss using ovine tendon collagen type I scaffold with skin cells. J Tissue Eng Regen Med 13:874–891. https://doi.org/10.1002/term.2842
23. El-Meliegy E, Abu-Elsaad NI, El-Kady AM, Ibrahim MA (2018) Improvement of physico-chemical properties of dextran-chitosan composite scaffolds by addition of nano-hydroxyapatite. Sci Rep 8:1–10. https://doi.org/10.1038/s41598-018-30720-2
24. Crowley LC, Marfell BJ, Christensen ME, Waterhouse NJ (2016) Measuring cell death by trypan blue uptake and light microscopy. Cold Spring Harb Protoc 2016:643–646. https://doi.org/10.1101/pdb.prot087155
25. Ozdemir E, Sendemir-Urkmez A, Yesil-Celiktas O (2013) Supercritical CO_2 processing of a chitosan-based scaffold: Can implantation of osteoblastic cells be enhanced? J Supercrit Fluids 75:120–127. https://doi.org/10.1016/j.supflu.2012.12.031
26. Number P, Reagents US (1801) Ready-to-use cell proliferation colorimetric reagent, WST-1 assay kit. 1:1800–1801
27. Dayı B, Bilecen DS, Eröksüz H et al (2021) Evaluation of a collagen-bioaggregate composite scaffold in the repair of sheep pulp tissue. Eur Oral Res 55:152–161. https://doi.org/10.26650/eor.20211911441
28. Fischer ER, Hansen BT, Nair V et al (2012) Scanning electron microscopy. Curr Protoc Microbiol 25:1–47. https://doi.org/10.1002/9780471729259.mc02b02s25
29. Internet manual downloaded from blyscan sulfated glycosaminoglycan assay general protocol. 1–17. https://www.biovendor.com/file/11574/blyscan-assay-manual-1-%20B1000.pdf
30. Labassaytm ALP. Code no: 291–58601. http://www.biotnt.com/file/BioTNTPDF/921@291-58601.pdf
31. Abarrategi A, Lópiz-Morales Y, Ramos V et al (2010) Chitosan scaffolds for osteochondral tissue regeneration. J Biomed Mater Res Part A 95:1132–1141. https://doi.org/10.1002/jbm.a.32912
32. Baysan G, Gunes OC, Turemis C et al (2023) Using loofah reinforced chitosan-collagen hydrogel based scaffolds in-vitro and in-vivo; healing in cartilage tissue defects. Materialia 31:101881. https://doi.org/10.1016/j.mtla.2023.101881
33. Zhang W, Zhang Y, Li X et al (2022) Multifunctional polyphenol-based silk hydrogel alleviates oxidative stress and enhances endogenous regeneration of osteochondral defects. Mater Today Bio 14:100251. https://doi.org/10.1016/j.mtbio.2022.100251
34. Chen J (2022) Recent development of biomaterials combined with mesenchymal stem cells as a strategy in cartilage regeneration. Int J Transl Med 2:456–481. https://doi.org/10.3390/ijtm2030035
35. Chen J Optimal properties of the scaffold. encyclopedia. https://encyclopedia.pub/entry/26952. Accessed 01 Feb 2024
36. Chen X, Qi Y, Zhu C, Wang Q (2019) Effect of ultrasound on the properties and antioxidant activity of hawthorn pectin. Int J Biol Macromol 131:273–281. https://doi.org/10.1016/j.ijbiomac.2019.03.077
37. Al-Moghrabi RS, Abdel-Gaber AM, Rahal HT (2018) A comparative study on the inhibitive effect of Crataegus oxyacantha and Prunus avium plant leaf extracts on the corrosion of mild steel in hydrochloric acid solution. Int J Ind Chem 9:255–263. https://doi.org/10.1007/s40090-018-0154-3
38. Moldovan B, David L, Achim M et al (2016) A green approach to phytomediated synthesis of silver nanoparticles using *Sambucus nigra* L. fruits extract and their antioxidant activity. J Mol Liq 221:271–278. https://doi.org/10.1016/j.molliq.2016.06.003
39. Mariychuk R, Porubská J, Ostafin M et al (2020) Green synthesis of stable nanocolloids of monodisperse silver and gold nanoparticles using natural polyphenols from fruits of *Sambucus nigra* L. Appl Nanosci 10:4545–4558. https://doi.org/10.1007/s13204-020-01324-y
40. Azhar FF, Olad A, Salehi R (2014) Fabrication and characterization of chitosan-gelatin/nanohydroxyapatite-polyaniline composite with potential application in tissue engineering scaffolds. Des Monomers Polym 17:654–667. https://doi.org/10.1080/15685551.2014.907621
41. Beck EC, Barragan M, Tadros MH, Gehrke SH, Detamore MS (2016) Approaching the compressive modulus of articular cartilage with a decellularized cartilage-based hydrogel. Acta Biomater 38:94–105. https://doi.org/10.1016/j.actbio.2016.04.019
42. Zhang B, Huang J, Narayan RJ (2020) Gradient scaffolds for osteochondral tissue engineering and regeneration. J Mater Chem B 8:8149–8170. https://doi.org/10.1039/d0tb00688b

43. Kim HN, Kang DH, Kim MS et al (2012) Patterning methods for polymers in cell and tissue engineering. Ann Biomed Eng 40:1339–1355. https://doi.org/10.1007/s10439-012-0510-y
44. Vo NTN, Huang L, Lemos H et al (2021) Genipin-crosslinked chitosan hydrogels: preliminary evaluation of the in vitro biocompatibility and biodegradation. J Appl Polym Sci 138:1–11. https://doi.org/10.1002/app.50848
45. Strauss FJ, Nasirzade J, Kargarpoor Z et al (2020) Effect of platelet-rich fibrin on cell proliferation, migration, differentiation, inflammation, and osteoclastogenesis: a systematic review of in vitro studies. Clin Oral Investig 24:569–584. https://doi.org/10.1007/s00784-019-03156-9
46. Jain KG, Mohanty S, Ray AR et al (2015) Culture & differentiation of mesenchymal stem cell into osteoblast on degradable biomedical composite scaffold: in vitro study. Indian J Med Res 142:747–758. https://doi.org/10.4103/0971-5916.174568
47. Ragetly G, Griffon DJ, Chung YS (2010) The effect of type II collagen coating of chitosan fibrous scaffolds on mesenchymal stem cell adhesion and chondrogenesis. Acta Biomater 6:3988–3997. https://doi.org/10.1016/j.actbio.2010.05.016
48. Danikowski KM, Cheng T (2019) Colorimetric analysis of alkaline phosphatase activity in s. Aureus biofilm J Vis Exp 2019:2–5. https://doi.org/10.3791/59285
49. Westhauser F, Karadjian M, Essers C et al (2019) Osteogenic differentiation of mesenchymal stem cells is enhanced in a 45S5-supplemented β-TCP composite scaffold: an in-vitro comparison of Vitoss and Vitoss BA. PLoS ONE 14:1–18. https://doi.org/10.1371/journal.pone.0212799
50. Katta J, Stapleton T, Ingham E et al (2008) The effect of glycosaminoglycan depletion on the friction and deformation of articular cartilage. Proc Inst Mech Eng Part H J Eng Med 222:1–11. https://doi.org/10.1243/09544119JEIM325
51. Hoemann CD, Sun J, Chrzanowski V, Buschmann MD (2002) A multivalent assay to detect glycosaminoglycan, protein, collagen, RNA, and DNA content in milligram samples of cartilage or hydrogel-based repair cartilage. Anal Biochem 300:1–10. https://doi.org/10.1006/abio.2001.5436
52. Alaqeel M, Grant MP, Epure LM et al (2020) Link N suppresses interleukin-1β-induced biological effects on human osteoarthritic cartilage. Eur Cells Mater 39:65–76. https://doi.org/10.22203/eCM.v039a04
53. Zhao F, Yin Y, Lu WW et al (2002) Preparation and histological evaluation of biomimetic three-dimensional hydroxyapatite/chitosan-gelatin network composite scaffolds. Biomaterials 23:3227–3234. https://doi.org/10.1016/S0142-9612(02)00077-7
54. Maji S, Agarwal T, Das J, Maiti TK (2018) Development of gelatin/carboxymethyl chitosan/nano-hydroxyapatite composite 3D macroporous scaffold for bone tissue engineering applications. Carbohydr Polym 189:115–125. https://doi.org/10.1016/j.carbpol.2018.01.104

Authors and Affiliations

Gizem Baysan[1] · Pinar Akokay Yilmaz[2] · Aylin Ziylan Albayrak[1,3] · Hasan Havitcioglu[1,4]

✉ Aylin Ziylan Albayrak
aylin.albayrak@deu.edu.tr

[1] Institute of Health Science, Department of Biomechanics, Dokuz Eylül University, 35340 Izmir, Turkey

[2] Department of Medical Laboratory Techniques, Izmir Kavram Vocational School, 35230 Izmir, Turkey

[3] Faculty of Engineering, Department of Metallurgical and Materials Engineering, Dokuz Eylül University, 35390 Izmir, Turkey

[4] Faculty of Medicine, Department of Orthopedics and Traumatology, Dokuz Eylül University, 35340 Izmir, Turkey